

ARTICLE OPEN



The effects of human movements on urban climate over Eastern China

Lingyun Wu¹ and Jingyong Zhang^{2,3}✉

We live on an urban planet with unprecedented human mobility. In this study, we collectively analyze ten large cities over densely populated Eastern China, and detect that mass people outflows during Spring Festival (SF) holiday significantly cool down urban climate expressed as urban heat island intensity variation particularly at the nighttime after minimizing the effects of other factors. We estimate that the average nighttime cooling effects of the ten large cities over Eastern China during the SF holiday relative to the nearby background period are 0.63 °C stronger during the 2000s than during the 1990s. The attribution analysis points to that the urban cooling effects are primarily caused by mass people outflows during the SF holiday. Our findings help to better understand the complex interactions of human population dynamics, urban development, and the environment, and may have important implications for promoting sustainable, people-centered, and resilient development of our urban planet.

npj Urban Sustainability (2021)1:36; <https://doi.org/10.1038/s42949-021-00038-6>

INTRODUCTION

The number of global human population has reached up to around 7.7 billion in 2019 with a further expected increase to nearly 10 billion by 2050¹. In the increasingly populous, interlinked and urbanized world, people mobility is reshaping the human society and the urban planet. Mainly due to rapidly growing movements from rural communities to urban areas, 55% of the total population in the world—4.2 billion people—resided in cities in 2018². As the most noticeable rural-to-urban migration continues, more 2.5 billion urban dwellers are expected to add by 2050, with 35% of the growth occurring in just three countries including India, China, and Nigeria². Cities are at the center of social and economic development of the world, and also become main drivers of global energy consumption, greenhouse gas emissions and climate change^{3–9}. Managing urban growth with unprecedented human mobility to promote the benefits and opportunities of the agglomeration, while reduce adverse impacts on the environment and our society is key to sustainable development of the world now and in the future^{10–17}. However, it remains very challenging to assess what effects human mobility can have on urban climate and other aspects of the environment.

Urban dwellers live with, and affect urban climate through many ways. Densely concentrated human activities, largely consumed energy and man-made impervious surface cause higher urban temperature than surrounding environment—the Urban Heat Island (UHI)^{18–24}. The UHI magnitude usually reaches several degrees, and can occasionally warm up urban areas above 10 °C^{25–28}. UHI-induced warming is thought to substantially affect local-to-regional climate^{29–37}, and also contribute to present global temperature rise, which is exceeding 1.0 °C above pre-industrial levels^{38,39}. As the urbanization and the world's population continue to grow, intensified UHI effects are expected to pose increasingly warming-related risks on the human society and the urban planet^{40–43}. Humans depend strongly on, and interfere intensely with urban climate and environment, and the human-city nexus tends to be further strengthened in the future.

China is the largest country in terms of population size, and has witnessed unprecedented urbanization development in the human history during the past decades^{44–48}. China's total population reached 1.4 billion with around 900 million people living in urban areas in 2020, and the urban dwellers are expected to surpass 1 billion by 2030. Spring Festival (SF) is the most important holiday in China, and each year mass national population movements take place during the SF holiday. The number of passenger trips and journeys during the SF holiday was estimated to run into 1 billion in the early 1990s, and increased rapidly to 3 billion or more in the 2010s. The mass outflows of urban people from large cities lead to abruptly decreased human activities associated with largely reduced anthropogenic heat release and other affected processes, and may thus be noticeably influential to urban climate^{49,50}. Several recent case studies indeed demonstrated observational evidence for the SF human movement impacts on urban temperature and relative humidity of Chinese large cities^{51–56}.

The majority of floating people which are the main trigger of the SF mass population movements live in large cities over densely populated and economically developed Eastern China, especially concentrating in municipalities and provincial capital cities^{49,57}. Here, we systematically assess the effects of people movements on urban climate expressed as UHI intensity (UHII) variation during the SF holiday over Eastern China. Ten municipalities and provincial capital cities including Beijing, Tianjin, Shijiazhuang, Taiyuan, Zhengzhou, Shanghai, Hangzhou, Nanchang, Changsha, and Fuzhou are selected and analyzed for the period of 1990–2014, taking into account carefully the availability, quality, and reliability of station observations (see “Methods” section). In 2020, the ten large cities are home to over 126 million population, and account for above 15% of China's total gross domestic product (GDP) (Supplementary Table 1).

We detect collective effects of population outflows on urban surface air temperature relative to the nearby surroundings at the ten large cities over Eastern China by minimizing the roles of other

¹State Key Laboratory of Numerical Modeling for Atmospheric Sciences and Geophysical Fluid Dynamics (LASG), Institute of Atmospheric Physics, Chinese Academy of Sciences, 100029 Beijing, China. ²Center for Monsoon System Research, Institute of Atmospheric Physics, Chinese Academy of Sciences, 100029 Beijing, China. ³College of Earth and Planetary Sciences, University of Chinese Academy of Sciences, 100049 Beijing, China. ✉email: zjy@mail.iap.ac.cn

Table 1. Dates of Spring Festival (SF) day, the SF holiday period (15 days, including the first day to the fifteenth day of the first month in a Chinese year), and the non-SF background period (60 days including 45th days to 16th days before the SF day and 25th days to 54th days after the SF day).

Year	SF day	SF period (15 days)	Background period (60 days)
1990	January 27	January 27–February 10	December 13–January 11, February 21–March 22
1991	February 15	February 15–March 1	January 1–January 30, March 12–April 10
1992	February 4	February 4–February 18	December 21–January 19, February 29–March 29
1993	January 23	January 23–February 6	December 9–January 7, February 17–March 18
1994	February 10	February 10–February 24	December 27–January 25, March 7–April 5
1995	January 31	January 31–February 14	December 17–January 15, February 25–March 26
1996	February 19	February 19–March 4	January 5–February 3, March 16–April 14
1997	February 7	February 7–February 21	December 24–January 22, March 4–April 2
1998	January 28	January 28–February 11	December 14–January 12, February 22–March 23
1999	February 16	February 16–March 2	January 2–January 31, March 13–April 11
2000	February 5	February 5–February 19	December 22–January 20, March 1–March 30
2001	January 24	January 24–February 7	December 18–January 8, February 18–March 26
2002	February 12	February 12–February 26	December 29–January 27, March 9–April 7
2003	February 1	February 1–February 15	December 18–January 16, February 26–March 27
2004	January 22	January 22–February 5	December 8–January 6, February 16–March 17
2005	February 9	February 9–February 23	December 26–January 24, March 6–April 4
2006	January 29	January 29–February 12	December 15–January 13, February 23–March 24
2007	February 18	February 18–March 4	January 4–February 2, March 15–April 13
2008	February 7	February 7–February 21	December 24–January 22, March 4–April 2
2009	January 26	January 26–February 9	December 12–January 10, February 20–March 21
2010	February 14	February 14–February 28	December 27–January 25, March 7–April 5
2011	February 3	February 3–February 17	December 20–January 18, February 28–March 29
2012	January 23	January 23–February 6	December 9–January 7, February 17–March 18
2013	February 10	February 10–February 24	December 27–January 25, March 7–April 5
2014	January 31	January 31–February 14	December 17–January 15, February 25–March 26

processes (see “Methods” section). The SF mass human movements are driven primarily by the floating people, which have increased rapidly in recent years (Supplementary Table 2). Thus, we take the 1990s as the reference period with the least likely impacts, and calculate their differences with those during 2000s and 2005–2014. Finally, we perform attribution analysis of urban coolings to mass people outflows during the SF holiday.

RESULTS

The effects of SF human movements on urban climate

Large cities over Eastern China have increasingly attracted the floating people from rural areas and smaller cities in the past decades. Most of the floating people or migrant workers in these large cities tend to leave for their native place during the SF holiday, which is the most precious family reunion time. We define the SF day to Lantern Festival as the SF holiday period, and choose 60 days including the 45th days to the 16th days before the SF day, and the 25th days to the 54th days after as the non-SF background period (Table 1). The UHII was calculated as surface air temperature difference between urban and non-urban reference stations for each large city (Fig. 1 and Supplementary Table 3). Then, the daily UHII anomalies were obtained by removing the daily UHII climatological values of all years. The trends in the differences of UHII anomalies between the SF holiday and the non-SF background period are used to assess the effects of human population movements on urban temperature. Details of data sources and statistical analysis are provided in the “Methods” section.

We find that the UHII anomalies during the SF holiday with regard to the nearby non-SF background period all show the

cooling trends for the ten large cities over Eastern China, with magnitudes ranging from -0.1 to -0.56 °C per decade for the study period in terms of mean surface air temperature (Supplementary Fig. 1 and Supplementary Table 4). Especially, the cooling trends have stronger magnitudes of -0.14 to -0.70 °C per decade during the night-time.

Collectively, the averaged cooling trends of urban daily mean, maximum, and minimum surface air temperatures in the SF holiday are -0.30 , -0.14 , and -0.43 °C per decade for the ten large cities over Eastern China during 1990–2009, and are all significant at the 95% confidence level (Supplementary Table 4). In comparison, the cooling effect is much stronger during the nighttime than the daytime. Among the ten large cities, the urban station of Shijiazhuang and the urban and non-urban stations of Taiyuan have relatively large relocations (>5 km) during the 2010–2014 (Supplementary Table 3). We excluded the two cities and perform the trend analysis for other eight large cities to assess the urban cooling effects of people outflows during 1990–2014. The cooling trends in the SF holiday are -0.28 and -0.40 °C per decade for urban daily mean and minimum surface air temperatures, both significant at the 99% confidence level (Supplementary Table 4). Ten-year moving averages to reduce the effects of interannual variations are further conducted, and the results show that the cooling effects of people outflows are much larger in recent years over Eastern China, especially for the night-time (Supplementary Fig. 2).

The urban cooling effects during different periods

China’s population was urbanizing rapidly during the study period, with urbanization rate increasing from 26.41% in 1990 to 54.77% in 2014 (Supplementary Table 2). Comparatively, large cities have

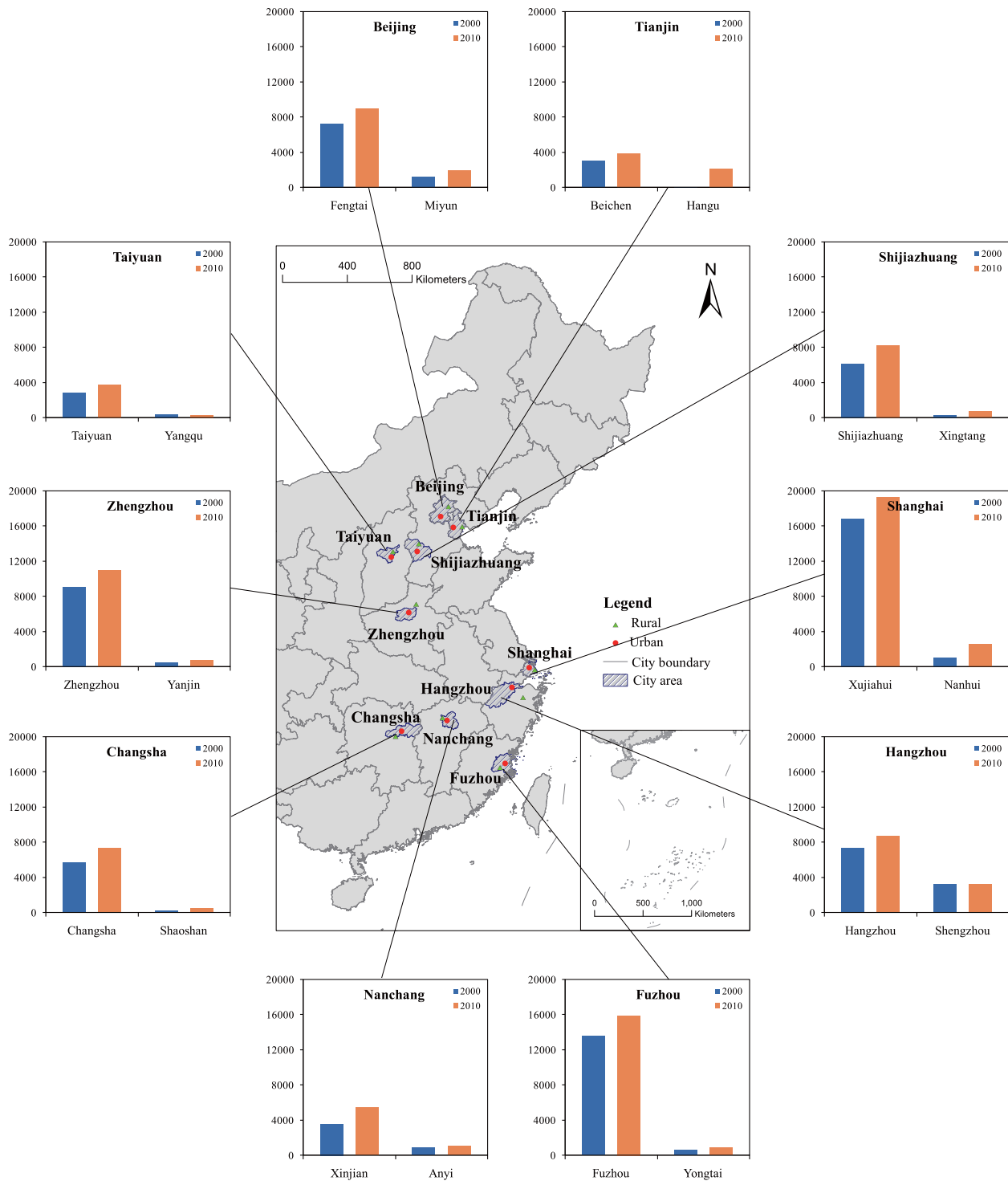


Fig. 1 Urban and nearby non-urban reference stations for ten large cities over Eastern China. All cities are municipalities or provincial capital cities, including Beijing, Tianjin, Shijiazhuang, Taiyuan, Zhengzhou, Shanghai, Hangzhou, Nanchang, Changsha, and Fuzhou. The bar charts show the population densities in 2000 and 2010 for urban and nearby non-urban reference stations. Map was generated using ArcGIS 10.2 (www.esri.com/software/arcgis).

experienced accelerating urbanization since around 2000 according to China's urbanization policies⁴⁷. The average annual rate of increased urban population was estimated at 1.33% during 2000–2014, which was more than 0.4% higher than that of the 1990s (Supplementary Table 2). The floating population increased from 37.5 million in 1990 to 102 million in 2000, and then rose up

rapidly to 221 million in 2010 and 253 million in 2014 (Supplementary Table 2). As a consequence, human population movements were much greater during the 2000s and 2010s than during the 1990s. Therefore, we take the 1990s as the reference period, which represents the least likely impacts of human movements on urban climate during the SF holiday, and further

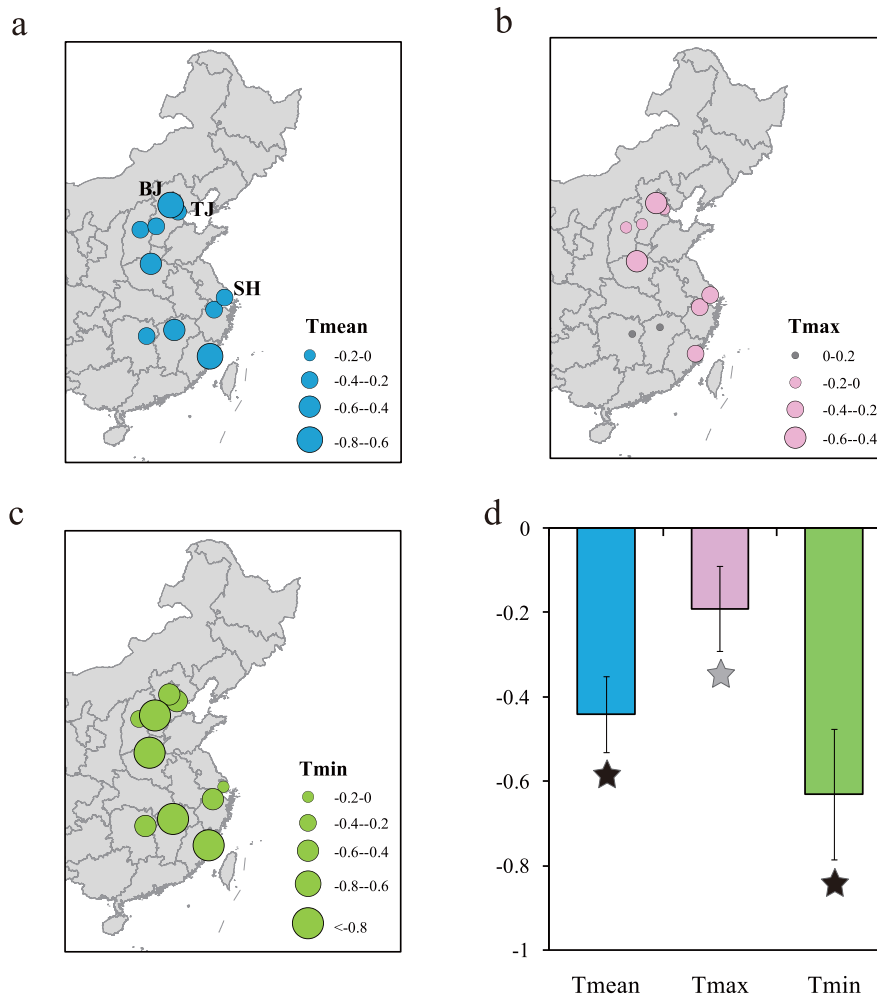


Fig. 2 Urban cooling effects of people outflows during the SF holiday period. Urban temperature variations during the SF holiday period for the 2000s (2000–2009) relative to the reference period of 1990s (1990–1999) for ten large cities over Eastern China: **a** daily mean surface air temperature (T_{mean}). **b** Daily maximum surface air temperature (T_{max}). **c** daily minimum surface air temperature (T_{min}). **d** T_{mean} , T_{max} , and T_{min} averaged over ten large cities. Urban temperature variations are characterized by the differences in the UHI anomalies between the SF holiday period and the non-SF background period. The gray and black stars in **d** represent the 95 and 99% confidence levels, respectively. The ± 0.5 standard deviations are also shown in **d**. Map was generated using ArcGIS 10.2 (www.esri.com/software/arcgis).

estimate the urban cooling effects during the 2000s relative to the 1990s baseline for the ten large cities over Eastern China (Fig. 2 and Supplementary Table 5).

The averaged cooling effects characterized as urban daily mean surface air temperature during the SF holiday relative to the non-SF background period in the 2000s are much stronger than those in the 1990s for all ten large cities, ranging from -0.25 to -0.79 °C. The nighttime cooling effects during the 2000s with respect to the 1990s vary at magnitudes of -0.17 to -1.06 °C for ten large cities.

Collectively, the averaged urban cooling effects during the 2000s relative to the 1990s baseline in terms of daily mean, maximum and minimum temperatures for the ten large cities over Eastern China are -0.44 , -0.19 , and -0.63 °C, and they are all significant at the 95% confidence level. During the cold season, energy consumptions for heating are much higher over Northern China than over Southern China. The averaged cooling effects during the 2000s relative to the 1990s are -0.45 , -0.26 , and -0.65 °C for five cities over Northern China (Beijing, Tianjin, Shijiazhuang, Taiyuan, and Zhengzhou) for daily mean, maximum, and minimum temperatures, while they are -0.43 °C, -0.13 °C, and -0.62 °C for five cities of Southern China (Shanghai, Hangzhou, Nanchang, Changsha, and Fuzhou). We also examine

the averaged cooling effects during the 2005–2014 relative to the 1990s for eight large cities, which have no relocations or small relocations during the whole study period of 1990–2014. The averaged urban cooling effects during the 2005–2014 relative to the 1990s in terms of the daily mean, maximum, and minimum temperatures are -0.52 °C, -0.22 °C, and -0.73 °C, and they are significant at the 99%, 95%, and 99% confidence levels, respectively (Supplementary Table 6). Together, these results highlight the significant cooling effects of population outflows on urban climate during the SF holiday over Eastern China.

The dependence of urban coolings on the floating population

Beijing, Tianjin, and Shanghai municipalities rank the top three most densely populated cities in China, and have the floating population data we can access (Supplementary Table 7). Here we further take these three large cities to explore the dependence of the urban coolings on the floating people, which are the main trigger of mass human movements during the SF holiday (Fig. 3). The results show that the floating people all had rapidly increased in recent years, accompanying with continuously remarkable decreases in urban temperature during the SF holiday over the three selected large cities. The R^2 values of the linear fits for urban

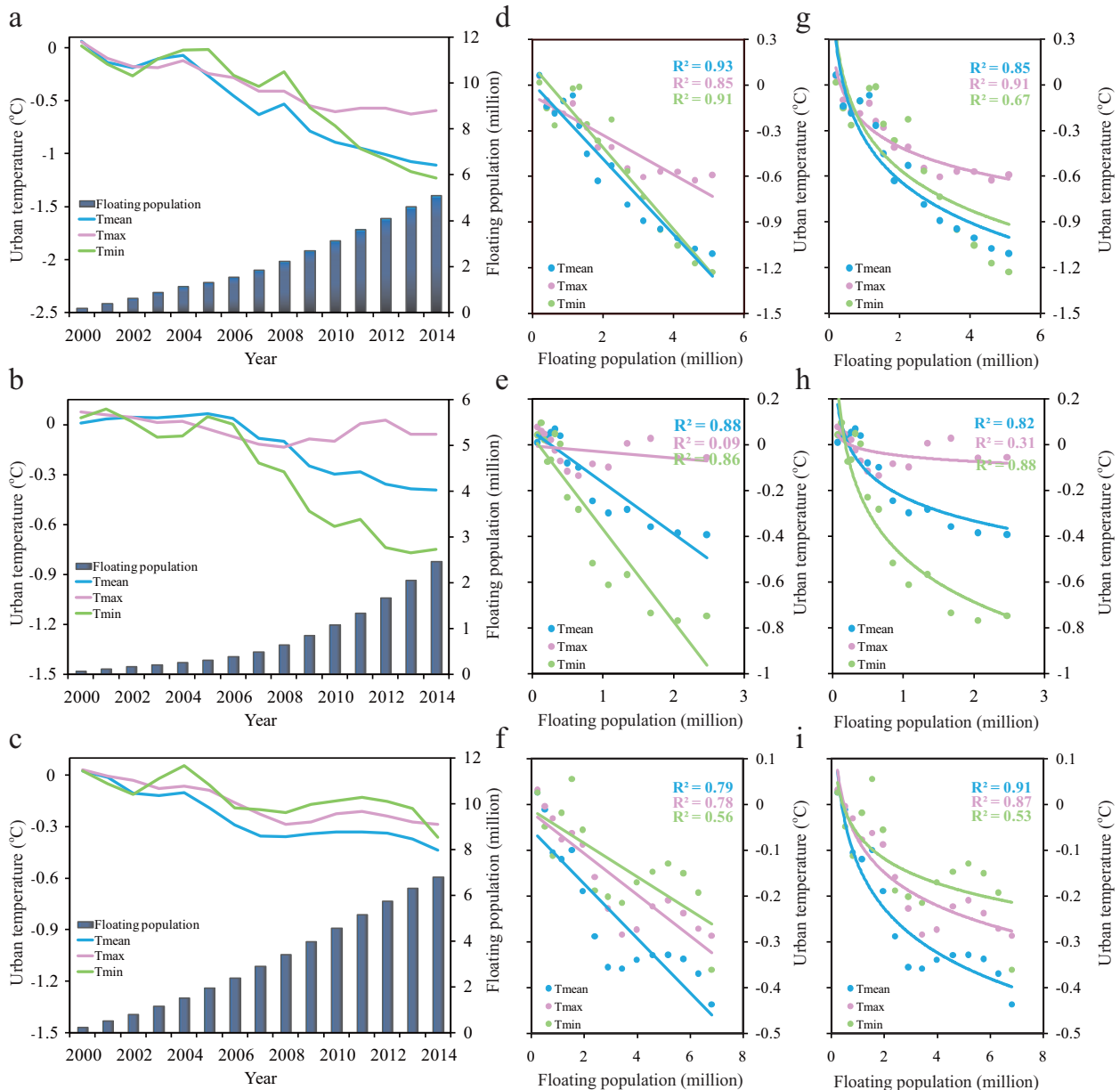


Fig. 3 Dependences of urban temperature variations during the SF holiday on the floating people. The upper, middle, and lower panels represent Beijing, Tianjin, and Shanghai municipalities, respectively. **a–c** show temporal variations of floating population and the differences in UHI anomalies between the SF holiday period and the non-SF background period in daily mean, maximum, and minimum surface air temperatures (T_{mean} , T_{max} , and T_{min}) in three selected large cities; **d–f** and **g–i** denote the linear and logarithmic fits of urban daily mean, maximum and minimum surface air temperatures variations to the floating people, respectively. To minimize the effects of interannual variations, the 10-year moving average is applied to all the data. The value in 2000 represents the 1991–2000 average relative to that of the 1990s (1990–1999) baseline period, and so on.

daily mean temperature variations to the floating people are all high (Table 2, 79–93%), pointing to that the urban coolings during the SF holiday are primarily induced by mass people outflows. The tight couplings between urban temperature variations during the SF holiday and the floating people are also evident via the linear fits for daily maximum and minimum temperatures. Using logarithmic fits, we also detect the strong couplings of urban temperature decreases during the SF holiday with the floating people (Table 2).

Abruptly decreased human activities induced by mass people outflows can lead to large reductions of energy consumptions and anthropogenic heat releases, thus causing the remarkable urban

Table 2. R^2 value for linear fitting (logarithmic fitting) of the urban temperature variations during the SF holiday to the floating people.

	T_{mean}	T_{max}	T_{min}
Beijing	0.93 ^a (0.85 ^a)	0.85 ^a (0.91 ^a)	0.91 ^a (0.67 ^a)
Tianjin	0.88 ^a (0.82 ^a)	0.09 (0.31 ^b)	0.86 ^a (0.88 ^a)
Shanghai	0.79 ^a (0.91 ^a)	0.78 ^a (0.87 ^a)	0.56 ^a (0.53 ^a)

^aSignificant at the 99% confidence level.

^bSignificant at the 95% confidence level.

coolings^{49,50,55}. A recent study demonstrated that sudden and large drops of energy consumptions and associated CO₂ emissions occurred during the SF holiday over China⁵⁸. Based on these analyses above together with our and other previous studies, the notable urban coolings of large cities over Eastern China during the SF holiday can be attributed primarily to the effects of mass people outflows via reducing the anthropogenic heat emissions and modulating the other processes.

DISCUSSION

Mass migration towards cities has reshaped our planet into the urban era. Deepening scientific understanding and enhancing effective managements of accelerated people movements, and their impacts play a particularly vital role in transforming the urban planet to a world of sustainable development in the Anthropocene^{59,60}. However, little attention has been paid to the role that human mobility can play in reshaping urban climate.

Taking the peculiar opportunity of the greatest periodic SF human movements, we reveal the remarkable cooling effects of mass population outflows during the SF holiday relative to the non-SF background period in ten typical large cities over Eastern China. The cooling effects averaged over the ten large cities during the 2000s relative to the 1990s are -0.44 , -0.19 , and -0.63 °C for daily mean, maximum, and minimum temperatures, which are all significant at the 95% confidence level. The much larger cooling effects of mass people outflows during the nighttime than during the daytime are expected, since the UHIs usually have remarkably stronger magnitudes at night. The averaged cooling effect for five large cities located over Northern China are larger than those of five cities over Southern China for all three temperature variables, which is in line with more energy consumptions for heating over Northern China. The urban coolings are well coupled with the floating population, and can be attributed primarily to people movement effects.

Collectively, our findings highlight the vital importance of human mobility to urban climate. Additionally, mass human movements to cities can worsen air quality, rise GHG emissions, and generate more wastes and noise among others, posing unprecedented environmental pressures on urban systems^{61–65}. These issues are all vital and need to be addressed in the future.

Meanwhile, human population dynamics, urban systems, and other specific local and regional contexts are highly complex and diverse. Further efforts are needed to reduce the uncertainties of our estimates and better elucidate the underlying mechanisms for the people movement effects on urban climate. For example, it is very difficult to choose appropriate urban and non-urban stations for Chinese large cities due to rapid urbanization over the past decades, and the non-urban surroundings also experienced the people outflows to some degree during the SF holiday. The observations from dense automatic weather stations should be used in future, and may be able to reduce the biases of our estimates.

A portfolio of strategies and approaches such as increasing green space and ecological corridors, improving energy efficiency, and deploying clean and renewable energy can produce multiple co-benefits such as reduced UHI effects, improved air quality and decreased greenhouse gas emissions^{10,11,66}. In the coming decades, the number, areas, and population of urban settlements will continue to grow rapidly, particularly in the global south¹³. Special attentions should be paid to the collaborative development of large, medium, and small cities, taking into consideration local, regional and global contexts in an integrated and systematic way^{9,67}.

We have entered a new era of unprecedentedly growing human mobility. Except for rural-to-urban movements, the international migrants have risen from 153 million in 1990 to around 272 million in 2019⁶⁸. In Europe and Northern America,

international migrants currently account for more than 10% of the total population. With easier and faster transportation, the international tourist arrivals have grown noticeably from 278 million in 1980 to 1451 million in 2018⁶⁹. Better understanding the complex interactions of human movements, urban systems, and the environment across various space and time scales provides critical scientific information for policy makers, private sectors, and other actors to successfully implement and achieve the New Urban Agenda and several key Sustainable Development Goals of the United Nations^{70,71}.

METHODS

Data

In this analysis, the daily mean, maximum, and minimum surface air temperature data were obtained from the China Meteorological Administration (<http://data.cma.cn/>[2020-01-24]).

The data of population, GDP, and percentage of tertiary industry in Supplementary Table 1 were achieved from Beijing Municipal Bureau of Statistics (<http://tj.beijing.gov.cn/EnglishSite/>[2021-06-20]), Tianjin Municipal Bureau of Statistics (<http://stats.tj.gov.cn/>[2021-06-20]), Shijiazhuang Municipal Bureau of Statistics (<http://tj.sjz.gov.cn/>[2021-06-20]), Taiyuan Municipal Bureau of Statistics (<http://stats.taiyuan.gov.cn/>[2021-06-20]), Zhengzhou Municipal Bureau of Statistics (<http://tj.zhengzhou.gov.cn/>[2021-06-20]), Shanghai Municipal Bureau of Statistics (<http://tj.sh.gov.cn/>[2021-06-20]), Hangzhou Municipal Bureau of Statistics (<http://tj.hangzhou.gov.cn/>[2021-06-20]), Nanchang Municipal Bureau of Statistics (<http://tj.nc.gov.cn/>[2021-06-20]), Changsha Municipal Bureau of Statistics (<http://tj.changsha.gov.cn/>[2021-06-20]), Fuzhou Municipal Bureau of Statistics (<http://tj.fuzhou.gov.cn/>[2021-06-20]), and National Bureau of Statistics of China (<http://www.stats.gov.cn/>[2021-06-20]). The urbanization rate and floating population data in Supplementary Table 2 were obtained from National Bureau of Statistics of China (<http://www.stats.gov.cn/english/>[2021-06-20]).

The population density in 2000 and 2010 over Eastern China at a spatial resolution of 30 arc second were taken from Shen et al.⁷² (data file S2 of supplementary material, <http://advances.sciencemag.org/cgi/content/full/3/7/e1700300/DC1/>[2020-01-24]). The data of resident and floating population during the period of 1990–2014 for Beijing, Shanghai, and Tianjin were collected from Beijing Municipal Bureau of Statistics (<http://nj.tj.beijing.gov.cn/nj/main/2015-tjnj/zk/indexch.htm/>[2021-01-04]), Shanghai Municipal Bureau of Statistics (<http://tj.sh.gov.cn/tjnj/nje15.htm?d1=2015tjnj/E0201.htm/>[2021-01-04]), and Tianjin Municipal Bureau of Statistics (<http://stats.tj.gov.cn/nianjian/2005nj/d2/2n2.htm/>[2021-01-04] for 1990–2004, <http://stats.tj.gov.cn/nianjian/2015nj/zk/indexch.htm/>[2021-01-04] for 2005–2014), respectively. Supplementary Table 7 provides floating population information for Beijing, Tianjin, and Shanghai municipalities for the period of 1990–2014.

Spring Festival holiday period and the non-Spring Festival background period

In the lunar calendar, the first day of the first month is called SF in China, and it falls on a different date each year in the solar calendar (Table 1). Traditionally, people celebrate the SF holiday from the SF day to Lantern Festival (the first day to the fifteenth day of the first month in a Chinese year). We therefore define the fifteen days as the SF holiday period. The annual mass people migration generally occurs during 40 days with starting at the 15th days before and ending on the 24th days after the SF day—Spring Festival Transportation (SFT) period. After excluding the SFT period, we select 60 days as the non-SF background period which includes the 45th days to the 16th days before the SF day, and the 25th days to the 54th days after (Table 1).

Ten large cities over Eastern China

The definitions and classification of cities vary across countries and regions. In 2014, Chinese government defines a city with the population living in core urban areas over 1 million as a large city (http://www.gov.cn/zhengce/content/2014-11/20/content_9225.htm/[2021-06-20]). The floating people which are the main trigger of SF mass human movements are mainly concentrated in densely populated and economically developed Eastern China, especially in municipalities and provincial capital cities^{49,57}. There are 15 municipalities and provincial capital cities including Beijing, Tianjin, Shijiazhuang, Taiyuan, Zhengzhou, Jinan, Nanjing, Hefei, Shanghai, Wuhan,

Hangzhou, Nanchang, Changsha, Fuzhou, and Guangzhou over Eastern China. According to the definitions and criteria established by Chinese government, the 15 cities are all classified as large cities.

For each large city, a pair of urban and non-urban reference stations were chosen according to the following criteria: (1) The two stations have no any relocations or only have small relocations (<5 km); (2) the two stations have consistent or similar climate background: the distance between two stations is shorter than 100 km, and the elevation difference is smaller than 120 m; (3) the two stations have obvious contrast in population condition: the population density difference between two stations is larger than 2000 person per km in 2000. The population density was calculated by averaging the values within 5 km circling each station. We used the tools of Buffer, Extract by Mask, and Zonal Statistics as Table in software of ArcGIS 10.2 to convert the population density data to the tabulated data (Supplementary Table 8). Note that the elevation difference of 120 m between urban and surrounding reference stations may cause a bias of above 0.5 °C in estimating the UHII. Such an effect can be largely removed in this study since we use relative change of the UHII.

Carefully taking into consideration the availability, quality, and reliability of the observational data judged by the above three criteria, ten large cities including Beijing, Tianjin, Shijiazhuang, Taiyuan, Zhengzhou, Shanghai, Hangzhou, Nanchang, Changsha, and Fuzhou were selected and analyzed among 15 municipalities and provincial capital cities over Eastern China for the period of 1990–2014 in this study. Figure 1 and Supplementary Table 3 present the locations and population densities of these urban and nearby non-urban reference stations of the selected ten large cities. The remaining five large cities (Jinan, Hefei, Nanjing, Wuhan, and Guangzhou) were excluded mainly due to stations relocations caused by such as rapid urbanization and land use management.

For each one of all the selected ten large cities over Eastern China, the amounts of the total and urban population are above 5 million and 4 million, respectively (Supplementary Table 1). The three municipalities of Beijing, Tianjin, and Shanghai all have urban population of exceeding 10 million. The ten large cities accounted for over 11% of China's total urban population, and over 15% of China's total GDP. The economies of the ten large cities are dominated by the tertiary industry.

Analysis

We assess the effects of mass human movements on urban climate of ten large cities (all for municipalities and provincial capital cities) over Eastern China during the SF holiday after minimizing the impacts of other factors⁵⁵. First, we calculated the surface air temperature difference (ΔT) between urban and nearby non-urban reference stations or UHII for each large city to separate the local urban effects because the UHII can minimize the impacts of large-scale or regional atmospheric circulation^{55,73}. Second, to reduce the impacts of the variability, the daily UHII anomalies were produced by subtracting the daily UHII climatological values of all years over a given period. Then, the differences in UHII anomalies (ΔT_{SF-BK}) between the SF holiday period and the non-SF background period were calculated, and we examined the trends of ΔT_{SF-BK} to detect urban temperature variations induced by mass people outflows over Eastern China (Supplementary Fig. 1 and Supplementary Table 4).

Since the human movements are much smaller during the first 10 years (1990s, 1990–1999) of the study period than during the following years, we estimated urban temperature changes induced by more mass human movements during the 2000s for ten large cities and during 2005–2014 for eight large cities by computing the differences with the reference period of 1990s (Fig. 2 and Supplementary Tables 5–6). Note that the resulting variations in urban temperature variables including daily mean, maximum, and minimum temperatures are relative to the surrounding non-urban values. We also calculated the 10-year moving values of ΔT_{SF-BK} relative to those for the 1990s baseline period (Supplementary Fig. 2). Finally, we performed attribution analysis by examining the dependence of urban temperature variations on the floating population, as the primary driver of mass people movements in three selected large cities including Beijing, Shanghai, and Tianjin municipalities using linear and logarithmic fits (Fig. 3 and Table 2).

DATA AVAILABILITY

The data used in this study, including population, GDP, and percentage of tertiary industry were all obtained from publicly available data with free accesses. The population density in 2000 and 2010 over Eastern China were taken from Shen

et al.⁷². The surface air temperature data were obtained from the China Meteorological Administration.

CODE AVAILABILITY

The code used to produce the results of this study is available from the authors upon reasonable request.

Received: 26 February 2021; Accepted: 1 September 2021;

Published online: 24 September 2021

REFERENCES

- United Nations, Department of Economic and Social Affairs, Population Division. *World Population Prospects 2019: Highlights*. http://population.un.org/wpp/Publications/Files/WPP2019_Highlights.pdf (UN, 2019).
- United Nations, Department of Economic and Social Affairs, Population Division. *World Urbanization Prospects: The 2018 Revision*. <https://population.un.org/wup/Publications/Files/WUP2018-KeyFacts.pdf> (UN, 2018).
- Grimm, N. B. et al. Global change and the ecology of cities. *Science* **319**, 756–760 (2008).
- Seto, K. C., Güneralp, B. & Hutrya, L. R. Global forecasts of urban expansion to 2030 and direct impacts on biodiversity and carbon pools. *Proc. Natl Acad. Sci. USA* **109**, 16083–16088 (2012).
- Gurney, K. R. et al. Track urban emissions on a human scale. *Nature* **525**, 179–181 (2015).
- Mcphearson, T. et al. Advancing urban ecology toward a science of cities. *BioScience* **66**, 198–212 (2016).
- Johnson, M. T. J. & Munshi-South, J. Evolution of life in urban environments. *Science* **358**, eaam8327 (2017).
- Acuto, M., Parnell, S. & Seto, K. Building a global urban science. *Nat. Sustain.* **1**, 2–4 (2018).
- Elmqvist, T. et al. Urbanization in and for the Anthropocene. *npj Urban Sustain.* **1**, 6 (2021).
- Bai, X. M. Six research priorities for cities and climate change. *Nature* **555**, 23–25 (2018).
- Kammen, D. M. & Sunter, D. A. City-integrated renewable energy for urban sustainability. *Science* **352**, 922–928 (2016).
- Krayenhoff, E. S. et al. Diurnal interaction between urban expansion, climate change and adaptation in US cities. *Nat. Clim. Change* **8**, 1097–1103 (2018).
- Nagendra, H., Bai, X. M., Brondizio, E. S. & Lwasa, S. The urban south and the predicament of global sustainability. *Nat. Sustain.* **1**, 341–349 (2018).
- Rodríguez, R. S., Ürge-Vorsatz, D. & Barau, A. S. Sustainable development goals and climate change adaptation in cities. *Nat. Clim. Change* **8**, 181–183 (2018).
- Rosenzweig, C. et al. Cities lead the way in climate-change action. *Nature* **467**, 909–911 (2010).
- Griggs, D. et al. Sustainable development goals for people and planet. *Nature* **495**, 305–307 (2013).
- World Tourism Organization. *UNWTO Annual Report 2017*. <https://www.e-unwto.org/doi/epdf/10.18111/9789284419807> (UNWTO, 2018).
- Oke, T. R. The energetic basis of the urban heat island. *Q. J. R. Meteorol. Soc.* **108**, 1–24 (1982).
- Arnfield, A. J. Two decades of urban climate research: a review of turbulence, exchanges of energy and water, and the urban heat island. *Int. J. Climatol.* **23**, 1–26 (2003).
- Oleson, K. W., Bonan, G. B., Feddema, J. & Jackson, T. An examination of urban heat island characteristics in a global climate model. *Int. J. Climatol.* **31**, 1848–1865 (2011).
- Ichinose, T., Shimodozono, K. & Hanaki, K. Impact of anthropogenic heat on urban climate in Tokyo. *Atmos. Environ.* **33**, 3897–3909 (1999).
- Li, D. et al. Urban island: aerodynamics or imperviousness? *Sci. Adv.* **5**, eaau4299 (2019).
- Yang, Q. Y., Huang, X. & Li, J. Y. Assessing the relationship between surface urban heat islands and landscape patterns across climatic zones in China. *Sci. Rep.* **7**, 9337 (2017).
- Yang, Q. Y., Huang, X. & Tang, Q. H. The footprint of urban heat island effect in 302 Chinese cities: temporal trends and associated factors. *Sci. Total Environ.* **655**, 652–662 (2019).
- Landsberg, H. E. Man-made climate change. *Science* **170**, 1265–1274 (1970).
- Peng, S. S. et al. Surface urban heat island across 419 global big cities. *Environ. Sci. Technol.* **46**, 696–703 (2012).
- Zhou, B., Rybski, D. & Kropp, J. P. The role of city size and urban form in the surface urban heat island. *Sci. Rep.* **7**, 4791 (2017).

28. Zhou, D. C. et al. The footprint of urban heat island effect in China. *Sci. Rep.* **5**, 11160 (2015).
29. Stewart, I. D. & Oke, T. R. Local climate zones for urban temperatures studies. *Bull. Am. Meteorol. Soc.* **93**, 1879–1900 (2012).
30. Taha, H. Urban climates and heat islands: albedo, evapotranspiration, and anthropogenic heat. *Energy Build.* **25**, 99–103 (1997).
31. Zhou, L. M. et al. Evidence for a significant urbanization effect on climate in China. *Pro. Natl Acad. Sci. USA* **101**, 9540–9544 (2004).
32. Kalnay, E. & Cai, M. Impact of urbanization and land-use change on climate. *Nature* **423**, 528–531 (2003).
33. Yang, Q. Q., Huang, X. & Li, J. Y. Assessing the relationship between surface urban heat islands and landscape patterns across climatic zones in China. *Sci. Rep.* **7**, 9337 (2017).
34. Zhao, L. et al. Interaction between urban heat islands and heat waves. *Environ. Res. Lett.* **13**, 034003 (2018).
35. Gu, Y. F. & Li, D. A modeling study of the sensitivity of urban heat islands to precipitation at climate scales. *Urban Clim.* **24**, 982–993 (2018).
36. Li, D. et al. Contrasting responses of urban and rural surface energy budgets to heat waves explain synergies between urban heat islands and heat waves. *Environ. Res. Lett.* **10**, 054009 (2015).
37. Zhao, L., Lee, X. H., Smith, R. B. & Oleson, K. Strong contributions of local background climate to urban heat island. *Nature* **511**, 216–219 (2014).
38. Intergovernmental Panel on Climate Change. *IPCC Sixth Assessment Report*. Global Warming of 1.5 °C, Special Report. <https://www.ipcc.ch/sr15/> (IPCC, 2018).
39. World Meteorological Organization. *WMO Statement on the State of the Global Climate in 2019*. https://library.wmo.int/index.php?lvl=notice_display&id=21700#.Xnr-kkq-tPY (WMO, 2020).
40. Gong, P. et al. Urbanisation and health in China. *Lancet* **379**, 843–852 (2012).
41. Zhao, L. Urban growth and climate adaptation. *Nat. Clim. Change* **8**, 1034–1036 (2018).
42. Levermore, G. et al. The increasing trend of the urban heat island intensity. *Urban Clim.* **24**, 360–368 (2018).
43. Yang, J. C., Hu, L. Q. & Wang, C. H. Population dynamics modify urban residents' exposure to extreme temperatures across the United States. *Sci. Adv.* **5**, eaay3452 (2019).
44. Bai, X. M., Shi, P. J. & Liu, Y. S. Realizing China's urban dream. *Nature* **509**, 158–160 (2014).
45. Yang, X. J. China's rapid urbanization. *Science* **342**, 310 (2013).
46. Wu, J. Urban ecology and sustainability: the state-of-the-science and future directions. *Landsc. Urban Plan.* **125**, 209–221 (2014).
47. Zhao, S. Q. et al. Spatial and temporal dimensions of urban expansion in China. *Environ. Sci. Technol.* **49**, 9600–9609 (2015).
48. Wu, J. G., Xiang, W. N. & Zhao, J. Z. Urban ecology in China: Historical developments and future directions. *Landsc. Urban Plan.* **125**, 222–233 (2014).
49. Manoli, G. et al. Magnitude of urban heat islands largely explained by climate and population. *Nature* **573**, 55–60 (2019).
50. Barbour, E. et al. Planning for sustainable cities by estimating building occupancy with mobile phones. *Nat. Commun.* **10**, 3736 (2019).
51. Zhang, J. Y., Wu, L. Y., Yuan, F., Dou, J. J. & Miao, S. Mass human migration and Beijing's urban heat island during the Chinese New Year holiday. *Sci. Bull.* **60**, 1038–1041 (2015).
52. Wu, L. Y., Zhang, J. Y. & Shi, C. X. Mass human migration and the urban heat island during the Chinese New Year holiday: a case study in Harbin City, Northeast China. *Atmos. Ocean. Lett.* **8**, 63–66 (2015).
53. Zhang, J. Y. & Wu, L. Y. Modulation of the urban heat island by the tourism during the Chinese New Year holiday: a case study in Sanya City, Hainan Province of China. *Sci. Bull.* **60**, 1543–1546 (2015).
54. Zhang, J. Y. & Wu, L. Y. The influence of population movements on the urban relative humidity of Beijing during the Chinese Spring Festival holiday. *J. Clean Prod.* **170**, 1508–1513 (2018).
55. Zhang, J. Y. & Wu, L. Y. Influence of human population movements on urban climate of Beijing during the Chinese New Year holiday. *Sci. Rep.* **7**, 45813 (2017).
56. Wu, L. Y. & Zhang, J. Y. Assessing population movement impacts on urban heat island of Beijing during the Chinese New Year holiday: effects of meteorological conditions. *Theor. Appl. Climatol.* **131**, 1203–1210 (2018).
57. Wei, S. & Wang, L. Examining the population flow network in China and its implications for epidemic control based on Baidu migration data. *Hum. Soc. Sci. Commun.* **7**, 145 (2020).
58. Liu, Z. et al. Near-real-time monitoring of global CO₂ emissions reveals the effects of the COVID-19 pandemic. *Nat. Commun.* **11**, 5172 (2020).
59. Keys, P. W. et al. Anthropocene risk. *Nat. Sustain.* **2**, 667–673 (2019).
60. Waters, C. N. et al. The Anthropocene is functionally and stratigraphically distinct from the Holocene. *Science* **351**, aad2622 (2016).
61. Mitchell et al. Long-term urban carbon dioxide observations reveal spatial and temporal dynamics related to urban characteristics and growth. *Proc. Natl. Acad. Sci. USA* **115**, 2912–2917 (2018).
62. Wigginton, N. S., Fahrenkamp-Uppenbrink, J., Wible, B. & Malakoff, D. Cities are the future. *Science* **352**, 904–905 (2016).
63. Jacobson, T. A. et al. Direct human health risks of increased atmospheric carbon dioxide. *Nat. Sustain.* **2**, 691–701 (2019).
64. Bouffanais, R. & Lim, S. S. Cities-try to predict superspreading hotspots for COVID-19. *Nature* **583**, 352–354 (2020).
65. Roches, S. D. Socio-eco-evolutionary dynamics in cities. *Evol. Appl.* **14**, 248–267 (2021).
66. Rosenzweig, C. et al. *Climate Change and Cities* (Cambridge University Press, 2018).
67. Forman, R. T. T. & Wu, J. G. Where to put the next billion people. *Nature* **537**, 608–611 (2016).
68. United Nations, Department of Economic and Social Affairs, Population Division. *International Migration 2019*. https://www.un.org/development/desa/pd/sites/www.un.org.development.desa.pd/files/files/documents/2020/Jun/international_migration_2019_report_june20.pdf (UN, 2019).
69. World Tourism Organization. *International Tourism Highlights, 2019 Edition*. <https://www.e-unwto.org/doi/epdf/10.18111/9789284421152> (UNWTO, 2019).
70. United Nations. *Transforming Our World: the 2030 Agenda for Sustainable Development A/RES/70/1*. <http://undocs.org/en/A/RES/70/1> (UN, 2015).
71. United Nations. *New Urban Agenda*. <http://undocs.org/en/A/RES/71/256> (UN, 2017).
72. Shen, H. Z. et al. Urbanization-induced population migration has reduced ambient PM_{2.5} concentrations in China. *Sci. Adv.* **3**, e1700300 (2017).
73. Zhou, L. M. et al. Impacts of wind farms on land surface temperature. *Nat. Clim. Change* **2**, 539–543 (2012).

ACKNOWLEDGEMENTS

This work was supported by the National Key Research and Development Program of China (2018YFA0606501, 2017YFA0603601) and the National Natural Science Foundation of China (Grant No.41675085).

AUTHOR CONTRIBUTIONS

J.Z. conceived the central idea. L.W. carried out the data analysis and prepared the figures. J.Z. and L.W. wrote the paper.

COMPETING INTERESTS

The authors declare no competing interests.

ADDITIONAL INFORMATION

Supplementary information The online version contains supplementary material available at <https://doi.org/10.1038/s42949-021-00038-6>.

Correspondence and requests for materials should be addressed to Jingyong Zhang.

Reprints and permission information is available at <http://www.nature.com/reprints>

Publisher's note Springer Nature remains neutral with regard to jurisdictional claims in published maps and institutional affiliations.



Open Access This article is licensed under a Creative Commons Attribution 4.0 International License, which permits use, sharing, adaptation, distribution and reproduction in any medium or format, as long as you give appropriate credit to the original author(s) and the source, provide a link to the Creative Commons license, and indicate if changes were made. The images or other third party material in this article are included in the article's Creative Commons license, unless indicated otherwise in a credit line to the material. If material is not included in the article's Creative Commons license and your intended use is not permitted by statutory regulation or exceeds the permitted use, you will need to obtain permission directly from the copyright holder. To view a copy of this license, visit <http://creativecommons.org/licenses/by/4.0/>.

© The Author(s) 2021